Food Chemistry: X 21 (2024) 101236

Contents lists available at ScienceDirect

Food Chemistry: X

journal homepage: www.sciencedirect.com/journal/food-chemistry-x

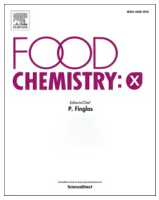

Study on antimicrobial activity of sturgeon skin mucus polypeptides (Rational Design, Self-Assembly and Application)

Beining Yang [a,b], Wei Li [c], Yuxuan Mao [d], Yuanhui Zhao [a,b], Yong Xue [a,b], Xinxing Xu [b], Yilin Zhao [a,b,*], Kang Liu [e,f,*]

[a] Sanya Oceanographic Institution /College of Food Science and Engineering, Ocean University of China, Sanya/Qingdao, China
[b] State Key Laboratory of Marine Food Processing & Safety Control, Ocean University of China, Qingdao, Shandong, China
[c] China Department of General Surgery, The District Hospital of Qingdao West Coast New Area, Qingdao, Shandong, China
[d] National Engineering Research Center for Wheat and Corn Deep Processing, College of Food Science and Engineering, Jilin Agricultural University, Changchun, Jilin, China
[e] College of Ocean Food and Biological Engineering, Jimei University, Xiamen, China
[f] National & Local Joint Engineering Research Center of Processing Technology for Aquatic Products, Xiamen, China

ARTICLE INFO

Keywords:
Sturgeon epidermal mucus
Antimicrobial peptide
Self-assembly
Molecular design
Antimicrobial activity

ABSTRACT

Despite the favorable biocompatibility of natural antimicrobial peptides (AMPs), their scarcity limits their practical application. Through rational design, the activity of AMPs can be enhanced to expand their application. In this study, we selected a natural sturgeon epidermal mucus peptide, AP-16 (APATPAAPALLPLWLL), as the model molecule and studied its conformational regulation and antimicrobial activity through amino acid substitutions and *N*-terminal lipidation. The structural and morphological transitions of the peptide self-assemblies were investigated using circular dichroism and transmission electron microscopy. Following amino acid substitution, the conformation of AL-16 (AKATKAAKALLKLWLL) did not change. Following *N*-terminal alkylation, the C_8-AL-16 and C_{12}-AL-16 conformations changed from random coil to β-sheet or α-helix, and the self-assembly changed from nanofibers to nanospheres. AL-16, C_8-AL-16, and C_8-AL-16 presented significant antimicrobial activity against *Pseudomonas* and *Shewanella* at low concentrations. *N*-terminal alkylation effectively extended the shelf life of *Litopenaeus vannamei*. These results support the application of natural AMPs.

1. Introduction

Increasing antibiotic resistance is a major concern driven by the overuse and incorrect use of antibiotics. It is associated with global public health risks as well as ecological and environmental risks (Nadgir & Biswas, 2023). The World Health Organization estimates that antibiotic resistance will result in 100,000 deaths globally by 2050 if it is not controlled or overcome (Pulingam, Parumasivam, Gazzali, Sulaimana, Chee, Lakshmanan, et al., 2022). Therefore, research into the development of alternative drugs and the generation of novel antimicrobial compounds are key focus areas.

Owing to the complexity and variability of their environment and constant exposure to pathogenic microorganisms, fish have developed various immune mechanisms. Epidermal mucus provides a first line of defense against aquatic microorganisms; it is rich in mucins and other adhesive colloids, and includes enzymes with antibacterial activity, such as proteases, AMPs, and lysozymes, which prevent the invasion of microorganisms (Dash, Das, Samal, & Thatoi, 2018).

The origins of sturgeon date back 200 million years to the Jurassic period (Bemis & Kynard, 1997). Currently, China farms sturgeons on the greatest scale globally (Yan, Dong, Dong, Song, Wang, & Hu, 2023). Fish epidermal mucus is a high-quality source for extracting natural AMPs; therefore, extracting and purifying AMPs from sturgeon epidermal mucus, and exploring their antibacterial effects and mechanisms of action, can enhance the added value of sturgeon.

AMPs typically comprise 12–50 amino acids with mixed hydrophobic and hydrophilic groups, thus allowing solubilization in both aqueous and lipid phases. Additionally, AMPs have a net positive charge of 2–9, with most adopting an amphiphilic structure when bound in membranes (Browne, Chakraborty, Chen, Willcox, Black, Walsh, et al., 2020).

* Corresponding authors at: Sanya Oceanographic Institution /College of Food Science and Engineering/State Key Laboratory of Marine Food Processing & Safety Control, Ocean University of China, Qingdao, Shandong, China (Y. Zhao).
E-mail address: zhaoyilin@ouc.edu.cn (Y. Zhao).

https://doi.org/10.1016/j.fochx.2024.101236
Received 4 January 2024; Received in revised form 11 February 2024; Accepted 15 February 2024
Available online 16 February 2024

Bacterial peptides destroy the integrity of the bacterial cell membrane, causing perforation and leakage. Furthermore, they can cross the cytoplasmic membrane without destroying its integrity, subsequently interacting with nucleic acids, affecting protein synthesis and inhibiting enzyme activity, thus, hindering cell division and attacking mitochondria (Saeed, Mergani, Aklilu, & Kamaruzzman, 2022). Thus, AMPs exert broad mechanisms of antimicrobial resistance, while it has less resistance induction, as this would require changes to the entire membrane structure or multiple biochemical pathways. These advantages make AMPs promising natural, non-toxic food additives that can be used in aquaculture, livestock food additives, or food preservatives (Magana, Pushpanathan, Santos, Leanse, Fernandez, Ioannidis, et al., 2020).

There are advantages of using AMPs as alternatives to antibiotics. However, the application of most natural AMPs for commercial application is limited owing to their low extraction efficiency, poor stability, and low economic benefits (Sarkar, Chetia, & Chatterjee, 2021). Furthermore, the development of AMPs as novel antibacterial agents is limited by their off-target toxicity (Rawson, Lacey, Strong, & Miller, 2022). Optimization of natural AMPs as templates can maximize antimicrobial activity while reducing cytotoxicity in mammals and overcoming the limitations of natural AMPs; these modified AMPs have potential as future drugs.

The antibacterial activity of AMPs is controlled by various factors, such as their net charge, hydrophobicity, and amphipathicity. These factors interact, and only when they are balanced can the maximum antibacterial effect be achieved (Tan, Fu, & Ma, 2021). Ye et al. (Ye & Aparicio, 2019) replaced alanine with a more hydrophobic amino acid in GL13K, a peptide capable of forming supramolecular self-assemblies, and obtained a peptide with enhanced antimicrobial potency. Additionally, coupling lipids or alkyl chains to natural AMPs can supplement their hydrophobic nature, resulting in amphiphilic peptides (PAs) with excellent nanostructures (Wang, Lu, Wang, Guo, Wu, Wan, et al., 2017). Similar to surfactant-like amphiphilic peptides, they possess the hydrophilicity of amino acids and the hydrophobicity of aliphatic long alkyl chains. The concept of amphiphilic peptides was first proposed by Kunitake et al (Kunitake, 1992). In aquatic environments, the hydrophobic alkyl tail undergoes self-aggregation similar to spontaneous protein folding (Zhong, Zhang, Zhu, Zhu, Yao, Gou, et al., 2021). Based on an understanding of the self-assembly mechanism, Yamamura et al. (Yamamura, Owaki, Isshiki, Ishihara, Kato, Katsu, et al., 2023) obtained cyclodextrin derivatives, similar to polymyxins, by connecting basic amino acids and hydrophobic alkyl chains to β-cyclodextrin molecules, which can selectively exert bacteriostatic effects and avoid adverse effects on red blood cells.

In our previous study, we extracted, purified, and identified an antibacterial peptide from sturgeon skin mucus, which has a structure of APATPAAPALLPLWLL (AP-16). In order to facilitate the application of antibacterial peptides in the preservation of aquatic products and inhibit the specific spoilage organism (*Pseudomonas* and *Shewanella*), in this study, we elucidated the impact of peptide structure and activity changes through rational design, characterization, and verification. The results support the development of novel antibacterial materials based on natural biological resources.

2. Materials and methods

2.1. Materials

Sturgeon was provided by Sturgeon Technology Co., Ltd. (Hangzhou, Zhejiang, China). AP-16 was isolated, purified, structurally identified, and synthesized from mucus scraped from the surface of sturgeon fish. Pseudomonas and Shewanella were provided by the China General Microbial Culture Collection Center. Human skin fibroblasts were provided by the Chinese Academy of Sciences. All other chemicals used in this work were analytical grade.

2.2. AMP synthesis

Target sequence peptides were synthesized using a fully automated microwave peptide synthesizer (Libertyl, CEM Company, America) based on Fmoc peptide solid-phase synthesis (SPPS), as described by Hussein et al (Hussein, Skwarczynski, & Toth, 2020; Winkler, 2020). This natural peptide was named AP-16 (APATPAAPALLPLWLL). AL-16 was synthesized by replacing proline with lysine. C_8-AL-16, C_{12}-AL-16, and C_{16}-AL-16 were obtained by attaching alkyl chains of different lengths to the *N*-terminus of AL-16.

2.3. Determination of purity and molecular weight

Synthetic peptides were purified using high-performance liquid chromatography (HPLC). A Globalsil GS-120–5-C18-BIO column (4.6*250 mm) was used with an injection volume of 10 μL. Mobile phase A was 0.1 % trifluoroacetic acid dissolved in 100 % acetonitrile and mobile phase B was 0.1 % trifluoroacetic acid dissolved in ultrapure water. The flow rate was 1.0 mL/min and the detection wavelength was 220 nm. The AMP was dissolved in sterile water at a concentration of 1 mg/mL, filtered through a 0.22 μm microporous filter membrane, and detected under the above chromatographic conditions.

The molecular mass of the synthesized peptides was determined using a matrix-assisted laser desorption ionization time-of-flight mass spectrometer (Microflex™ LRF, Bruker Daltonics, Germany). For MS experiments, a pulsed Nd: YAG laser with a wavelength of 355 nm was used at 100 Hz. The MS analysis was performed in positive and negative ion modes with an applied accelerating voltage of 19.0, reflection voltage of 20.0, accelerating voltage of 8 kV for MS/MS, pulsed ion extraction delay of 100 ns, and argon as the collision gas.

2.4. Circular dichroism

Samples were dissolved in sterile phosphate-buffered saline (PBS) and 2.5 % sodium dodecyl sulfate (SDS) buffer, filtered, and sterilized through a 0.22 μm microporous membrane to simulate the hydrophobic environment of cell membranes (Kocourkova, Novotna, St'ovickova-Habartova, Cujova, Cerovsky, Urbanova, et al., 2016). The secondary structures of AMPs in different environments were characterized using a J-815 circular dichroism chromatograph (JASCO, Japan). The scanning wavelength was 190–270 nm, the bandwidth was 1 nm, and the interval time was 0.5 s. Came with the instrument to obtain the ellipticity (θ) of the samples, which was converted to the molar residue ellipticity ([θ]) by using the formula:

$$[\theta] = \frac{\theta}{10\mathrm{ncl}}$$

where [θ] is the molar disability ellipticity in degrees•cm^2•dmol^{-1}; θ is the ellipticity in millidegree; n is the number of residues in the amphiphilic polypeptide; c is the concentration of amphiphilic peptide in mol/L (0.5 mol/L); and l is the optical range of the cuvette in cm (0.1 cm).

2.5. Transmission electron microscope

The self-assembled morphology of the AMPs was investigated using transmission electron microscopy (TEM) as described by Wang et al (Wang, et al., 2017). The sample concentration was 1 mM.

2.6. Functional activity and safety evaluation

The functional activity of peptides was defined as the minimum inhibitory concentration (MIC). As described by Al-Sarayreh et al. (Al-Sarayreh, Al-Shuneigat, Al-Saraireh, & Al-Qudah, 2021), the MIC was determined using a two-fold serial dilution method.

The safety of AMPs was evaluated based on their cytotoxicity.

Human skin fibroblasts were revived, passaged, and cultured until they reached the logarithmic growth phase, and the concentration was adjusted to 8×10^4 cells/mL. Wall-adherent cells were incubated at 37℃ and 5 % CO_2 for 24 h, supplemented with different concentrations of samples, and incubated for 20 h. Next, 10 μL Methylthiazolyldiphenyl-tetrazolium bromide (MTT) was added, cells were incubated for 4 h, and the supernatant was removed from the wells. Subsequently, 150 μL of dimethyl sulfoxide (DMSO) was added, and the absorbance at 490 nm was measured in each well after shaking for 15 min. Treatment without AMP was used as the negative control, and 150 μL of DMSO was used as the blank. Cell survival was calculated using the following formula:

$$\text{Cell viability}(\%) = \frac{A_{\text{peptide}} - A_{\text{blank control}}}{A_{\text{negative control}} - A_{\text{blank control}}} \times 100$$

2.7. Antimicrobial mechanism

2.7.1. Cell wall permeability

Samples were added to the bacterial solution to prepare solutions at the MIC (the negative control group was treated with the same volume of sterile water) and then placed in a 37℃ incubator for 4 h and centrifuged (4℃, 5000 × g) for 10 min. Subsequently, the supernatant was collected to determine the content of alkaline phosphatase (AKP) in the sample solution.

2.7.2. Cell membrane permeability

The integrity of the bacterial cell membrane was determined using flow cytometry to measure propidium iodide (PI) and fluorescein diacetate (FDA) uptake (Ajish, Yang, Kumar, & Shin, 2020). The turbidity of *Pseudomonas* and *Shewanella* grown to the logarithmic growth phase was adjusted to 0.4, after which bacteria were washed and resuspended in the same volume of sterile PBS. The samples were mixed with the bacterial solution to reach the MIC, and the mixture was then incubated at 37℃ (the optimal growth temperature) for 1 h. Subsequently, the samples were centrifuged (4℃, 5000 × g) for 10 min, the supernatant was discarded, and the cells were stained with PI/FDA solution for 20 min at 37℃, without light. Excess staining solution was discarded, and the cells were resuspended in PBS. The PBS-treated group served as a negative control. Finally, fluorescence was measured using a flow cytometer (BD FACSVerse™, Becton Dickinson and Company, USA).

2.7.3. Ultrastructural observations

The samples (bacterial cells treated with peptides) were sliced to 50–90 nm using a LEICA EM UC7 ultrathin sectioning machine and stained with lead nitrate and ethanol hydrogen peroxide acetate solution for 10 min each. Subsequently. the samples were visualized under a TEM, and images were captured by Digital Micrograph.

2.8. Extracellular protein leakage

Pseudomonas and *Shewanella* were cultured to logarithmic growth stage; then, an appropriate amount of bacterial solution was centrifuged (4℃, 5000 × g, 10 min), and the supernatant was discarded. The remaining bacterial precipitate was rinsed three times with PBS and resuspended. the same volume. The bacterial suspension was 1:1 mixed with the sample to obtain the MIC. The negative control group was added to the same volume of sterile water and incubated for 4 h before centrifugation. The supernatant was filtered through a 0.22 μm microporous filter membrane, and the amount of protein in the supernatant was quantified by BCA Protein Assay Kit (Solarbio, Beijing, Chian).

2.9. AMP application

Peptides with the greatest antibacterial activity were selected based on the above test results. The AMP solution was prepared according to the MIC and sterile water was used as a control. Shrimp were killed in ice water, washed with sterile water, drained, soaked for 30 min in AMP solution or sterile water at 4℃, and then stored in a sterile storage bag. The total bacterial count was calculated as described by Ambrosio (Ambrosio, Gogliettino, Agrillo, Proroga, Balestrieri, Gratino, et al., 2022), at a sampling interval of 1 day.

2.10. Statistical analysis

Each experiment was repeated at least three times. Results are expressed as the mean ± standard deviation (SD), statistical analyses were performed using SPSS statistics 22. Differences were considered statistically significant at $p < 0.05$.

3. Results and discussion

3.1. Characterization of the purity and molecular weight of AMPs

The purity of the synthesized peptides was verified using HPLC. As shown in the left column of **S.1.**, only one narrow peak was obtained at different times for each peptide. The purity of peptides was > 95 % based on calculation of the peak area, which was analyzed in the next step of the experiment.

S.1. and Table 1 showed the molecular weights of the peptides. The molecular weight of AP-16 was the smallest, at 1615.16 Da, while that of C_{16}-AL-16 was the largest, at 1964.2 Da. The molecular weights of all peptides were less than 2000 Da, and there was a high level of consensus between the actual and expected molecular weights. Based on the observed purity and molecular weights, the synthesized peptide was found to be the target peptide molecule and was used in further experiments. Fig. 1 showed the chemical structures of the five peptides. Through rational molecular design, modified peptides can contain positively charged amino acids or a high proportion of hydrophobic amino acids, ensuring their antibacterial effects via electrostatic or hydrophobic interactions.

3.2. Circular dichroism

When plane-polarized light passes through a medium containing chiral molecules such as proteins and peptides, left- and right-handed polarized light can develop; therefore, circular dichroism (CD) can be used to determine the configuration and conformation of these asymmetric molecules (Whitmore & Wallace, 2004). Stabilized secondary structures play a key role in the antimicrobial activity of AMPs (Takada, Ito, Kurashima, Matsunaga, Demizu, & Misawa, 2023). Three types of secondary structures can be obtained through circular dichroism, including α-Spiral structure (exhibiting characteristic negative peaks at 208 nm and 222 nm), β-Folding structure (positive peak at 195 nm and negative peak at 218 nm) and irregular curling (negative peak at around 195 nm and weak positive peak at 217 nm) (Spencer & Rodger, 2021).

As shown in Fig. 2 **(A)**, when the AMP was dissolved in an aqueous solution, AP-16 and AL-16 produced a negative peak near 197 nm and a weaker positive peak near 217 nm, indicating the formation of a randomly curled structure in aqueous solution. C_8-AL-16 produced a positive peak near 195 nm and a negative peak at 215 nm, forming a

Table 1
Molecular weight and purity of polypeptides.

Polypeptide	Theoretical Molecular weight (Da)	Actual molecular weight (Da)	Purity (%)
AP-16	1614.97	1615.16	96.72
AL-16	1739.2	1739.4	97.65
C_8-AL-16	1852.2	1865.44	95.82
C_{12}-AL-16	1908.2	1921.55	96.52
C_{16}-AL-16	1964.2	1977.65	96.26

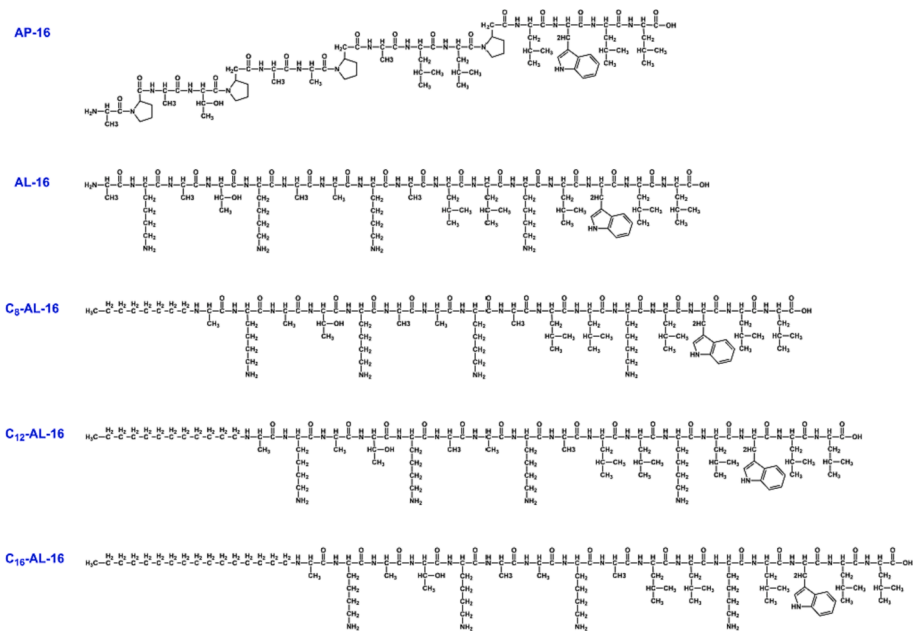

Fig. 1. Chemical structure of antimicrobial peptides.

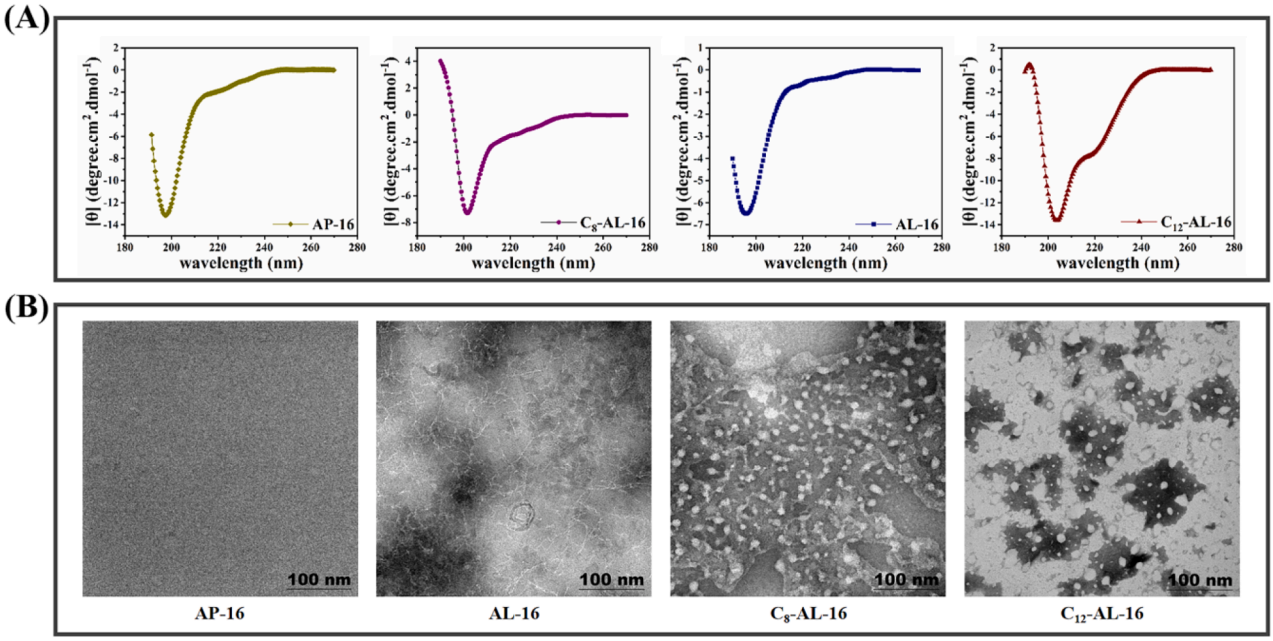

Fig. 2. Secondary structure of AMPs in H_2O (A) and self-assembly morphology of AMPs (B).

β-folded structure. Conversely, C_{12}-AL-16 produced a positive peak at 192 nm and negative peaks at 208 and 222 nm, forming an α-helix. This suggested that as the length of the alkyl chain added to the amino terminus of the antimicrobial peptide increased, the secondary structure of the AMP changed, forming typical β-folded and α-helical structures from the initial random curls. The α-helical and β-folded structures are important for antimicrobial activity (Pazderkova, Malon, Zima, Hofbauerova, Kopecky, Kocisova, et al., 2019). When an AMP comes into contact with a bacterium, it interacts with lipopolysaccharides (the main component of the extracellular membrane of the gram-negative bacterium) and folds, leading to a change in the secondary structure (Avitabile, D'Andrea, & Romanelli, 2014).

3.3. Self-assembly morphology

The secondary structure formed by non-covalent interactions between amino acids within the peptides considerably influences the supramolecular structure. Although the degree of change in the peptide molecules may be very small, the impact on the self-assembly structure could be substantial (Zhao, Li, Zhang, Wang, Wang, Wang, et al., 2020). As an ordered aggregate that can spontaneously form specific structures and functions, the antibacterial activity of self-assembling peptides linking lipid or alkyl chains can be greater than that of the original AMP sequence (Zhong, et al., 2021). The self-assembly morphology of the AMPs AP-16, AL-16, C_8-AL-16, and C_{12}-AL-16 in aqueous solution were shown in Fig. 2 **(B)**.

AP-16 did not exhibit an evident self-assembly morphology. AL-16 in aqueous solution exhibits a nanofiber structure that is typically resistant to dissociation into monomers. Consequently, this leads to a reduction in the concentration of functional monomers capable of exhibiting activity, thereby diminishing the overall activity level (Ma, Huang, Xie, Ma, Jia, Yao, et al., 2022). Changes in the morphology of C_8-AL-16 and C_{12}-AL-16 indicate that the addition of alkyl chains controls the self-assembly structure of the peptides. They self-assembled into nanospheres in the form of micelles. In self-assembled AMPs with lipid or alkyl chains, the assembly structure of peptides is primarily controlled by the "hydrophobic tail", while interactions between amino acids play a secondary role. Different nanostructures may result in significant differences in the antimicrobial activity of amphiphilic peptides. Generally, the antibacterial activity of closely packed micelles is greater than that of nanofibers, possibly because AMPs with micellar structures are prone to dissociation into monomers and direct insertion into bacterial membranes, leading to the leakage of bacterial contents (de Almeida, Han, Perez, Kirkpatrick, Wang, & Sheridan, 2019).

3.4. Evaluation of functional activity and safety

The antimicrobial activity of a peptide can be defined as its MIC, which is the lowest concentration that can inhibit the growth of a microorganism. The MIC of the peptides against *Pseudomonas* and *Shewanella* were shown in Fig. 3.

Following treatment with AP-16, the survival rates of both types of bacteria increased, and no significant antibacterial activity was demonstrated (**S.2.**), precluding further exploration of their properties. AL-16 presented a significant inhibitory effect on both types of bacteria, with MIC values of 16 μM (*Pseudomonas*) and 128 μM (*Shewanella*) (Fig. 3**A**). Following the addition of an alkyl chain to the *N*-terminus of AL-16, both C_8-AL-16 and C_{12}-AL-16 exhibited enhanced antibacterial activity, and the MIC decreased to 4 μM (Fig. 3**B,** Fig. 3**C**). Increasing the concentration of C_{12}-AL-16 enhances hydrophobicity. However, excessive hydrophobicity leads to increased inter-chain aggregation, resulting in a decline in antibacterial efficacy. This aligns with the findings of Song, W et al. (Song, Xin, Yu, Xia, & Pan, 2023) C_{16}-AL-16 demonstrated decreased antibacterial activity (**S.2**). The introduction of more positive charges through the substitution of amino acids accounts for these changes in peptide activity. When comparing AP-16 with AL-16, the net charge changed from 0 to +4. Enhancing the positive surface charge of a peptide can promote interactions with the cell membrane, thereby exerting more pronounced activity. Studies investigating AMPS from insects and other sources have demonstrated that a positive charge can facilitate the interaction of peptides with cell membrane lipopolysaccharides (Aschi, Perini, Bouchernal, Luzi, Savarin, Migliore, et al., 2020), thereby enhancing their activity. The addition of alkyl chains enhanced peptide hydrophobicity. Hydrophobic interactions can enhance the compactness of self-assembled structures and promote cell membrane binding, leading to membrane disruption and apoptosis induction. Overall, these results indicate that both amino acid substitutions and alkyl chain elongation positively affect the antimicrobial activity of the peptides.

Fig. 3 **(D, E, F)** presented the results of the cytotoxicity assays performed using different peptides. The three modified peptides did not exhibit significant cytotoxicity within their MIC range. Similarly, we evaluated the cytotoxicity of C_{16}-AL-16, and the results are shown in **S.2.** Compared to the MIC results, C_{16}-AL-16 exhibited significant cytotoxicity, rendering it unsuitable for practical application. Alkyl chains can enhance the antimicrobial activity of peptides; however, excessive length can also increase toxicity.

3.5. Antibacterial activity of peptides

To determine the antimicrobial activity of the peptides, we explored their effects on cell wall permeability, cell membrane permeability, and changes in bacterial cell morphology.

The results of bacterial cell wall permeability analyses following peptide treatment were shown in Fig. 4 **(A, B)**. The bacterial cell wall maintains cellular physiology and balances osmotic pressure, and its integrity is critical to cell viability and morphology (Garcia, Botet, Rodriguez-Pena, Bermejo, Ribas, Revuelta, et al., 2015). The presence of AKP between the cell wall and cell membrane of bacteria plays an important role in metabolism; AKP cannot pass through the cell wall without causing damage. However, when the bacterial cell wall is damaged, AKP leaks into the extracellular space. Therefore, AKP is used as a marker to assess cell wall permeability and integrity (OuYang, Duan, Li, & Tao, 2019). All three peptides had a significant impact on

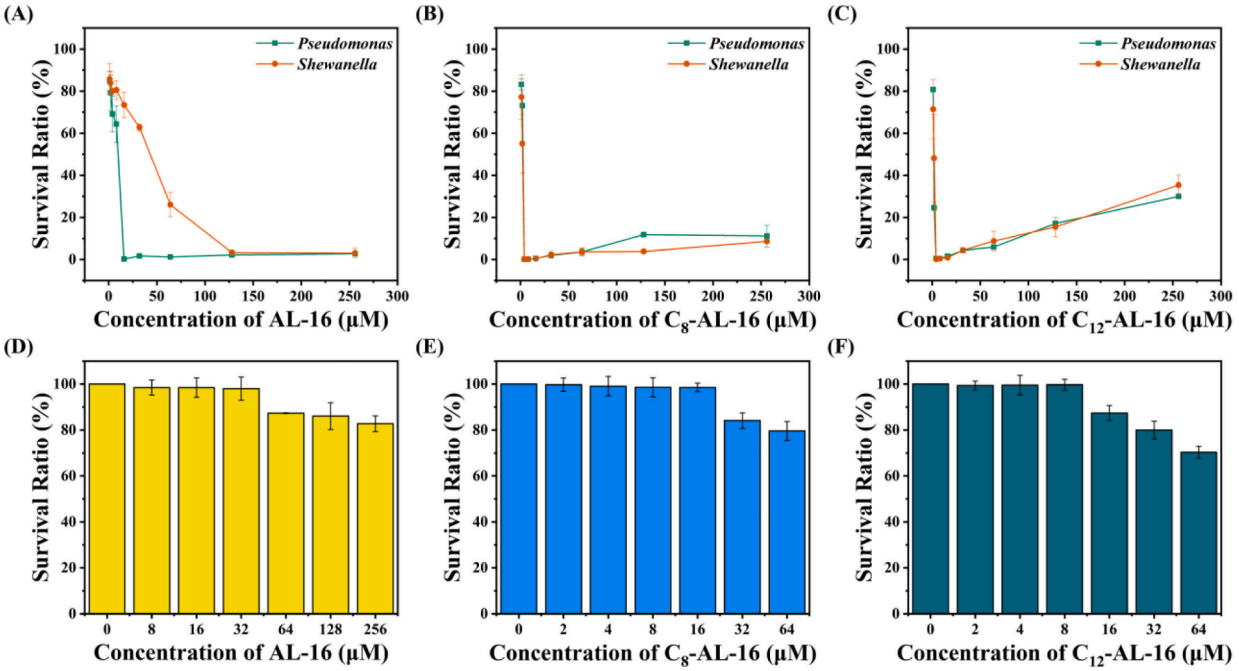

Fig. 3. Assessment of the antimicrobial activity and safety of different peptides.

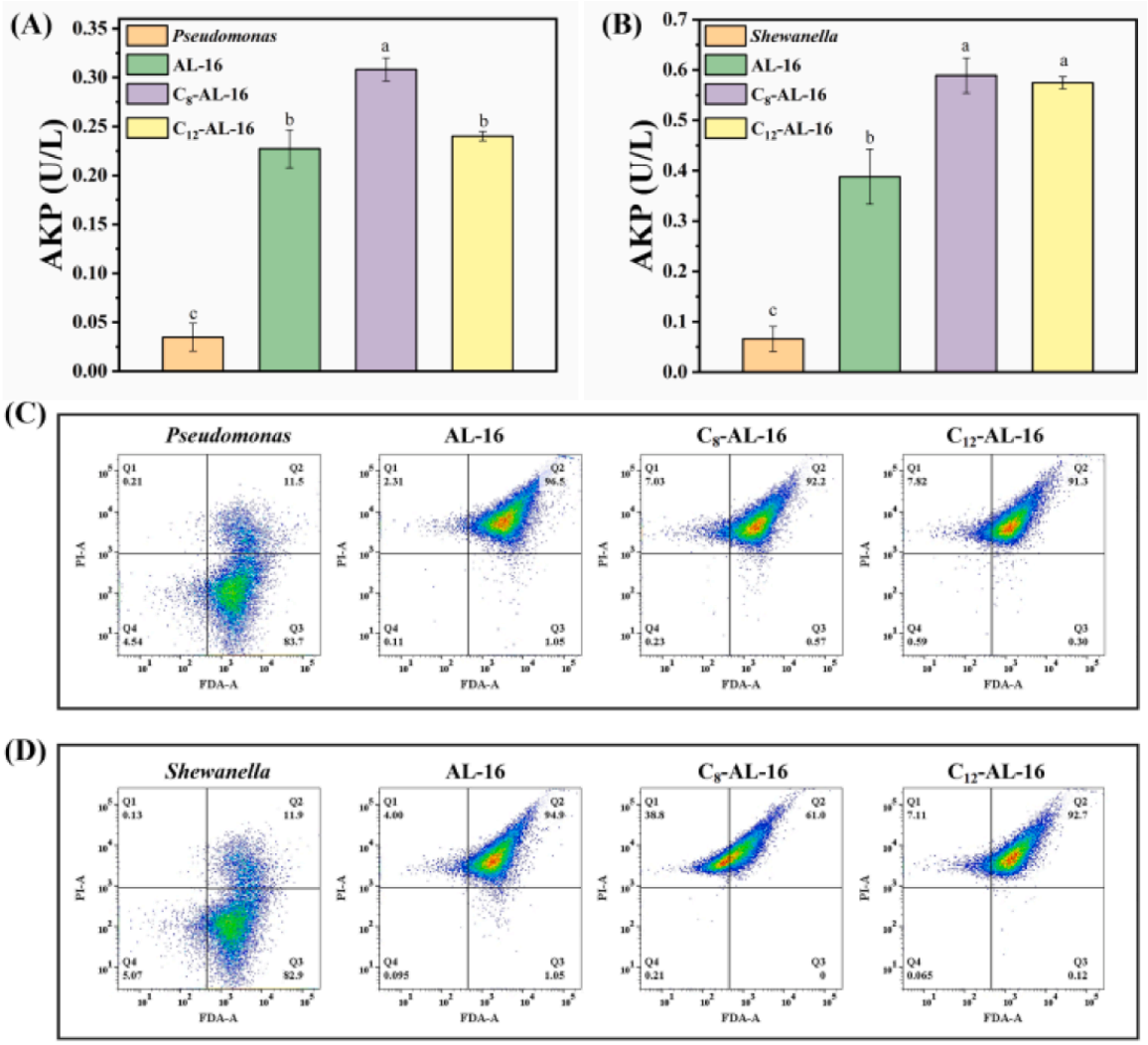

Fig.4. Assessment of bacterial cell wall and cell membrane integrity following peptide treatment.

bacterial cell wall. C_8-AL-16 significantly enhanced cell wall permeability of both bacterial strains, consistent with the antibacterial activity of the peptides.

PI is membrane-impermeable; it can only enter dead cells or those with damaged membranes. In cells with damaged membranes, PI embeds itself in the DNA, producing red fluorescence (Habtewold, Duchateau, & Christophides, 2016). FDA is a non-autofluorescent dye that freely penetrates intact cell membranes and is hydrolyzed by intracellular non-specific esterase enzymes to produce a luminescent luciferin that does not pass through the cell membrane. This accumulates inside the cell and emits green fluorescence (London, Contractor, Lake, Aucott, Bell, & James, 1990). Flow cytometry (FCM) can be used in conjunction with the fluorescent dye PI/FDA to differentiate and count live cells (Hiraoka & Kimbara, 2002). Fig. 4 **(C, D)** showed the impact of the peptides on bacterial cell membranes. The Q4 region is a PI-negative and FDA-positive region, representing cells with intact membranes and good intracellular enzyme activity; most of the *Pseudomonas* and *Shewanella* were distributed in this region following treatment with PBS (83.70 % and 82.90 %, respectively). The distribution region of bacteria incubated with AL-16, C8-AL-16, and C12-AL-16 showed significant changes ($P < 0.05$), mainly distributed in Q1 and Q2 regions (>98 %); the Q1 region was PI-positive and FDA-negative, in which the cell membranes were disturbed and no intracellular enzyme activity could be detected. The Q2 region was PI- and FDA-positive, in which the cells had disturbed membranes but detectable intracellular enzymatic activity. Thus, treatment with the three antimicrobial peptides disrupted the cell membrane integrity of *Pseudomonas* and *Shewanella*. In *Shewanella* treated with C_8-AL-16, 38.80 % were distributed in the Q1 region with severe disruption of the cell membrane, indicating its potent inhibitory activity.

Morphological changes in bacterial cells following peptide treatment were shown in Fig. 5**.** The cell structure of *Pseudomonas* in the control group was uniform; the cell membrane and cell wall were intact and smooth, and the contents were intact, indicative of a healthy state. Following treatment with AL-16 and C_{12}-AL-16, the bacterial contents were lost; however, the basic membrane structure was maintained. The cell membrane of *Pseudomonas* treated with C_8-AL-16 was disrupted by lysis, and the contents leaked, resulting in serious damage. Some bacterial cytoplasm was lost following AL-16 treatment, and while the membrane surface was crumpled, the long rod-like structure was maintained. The surface of bacteria treated with C_8-AL-16/C_{12}-AL-16 shrunk, the cell wall and cytoplasm separated, intracellular material leaked, cell membrane lost selective permeability, the cell swelled and deformed, and the membrane was ruptured. Furthermore, the cytoplasm almost completely leaked or decomposed into cellular fragments.

3.6. Leakage of extracellular protein

As shown in Fig. 6, the extracellular protein content of *Pseudomonas* and *Shewanella* increased significantly upon the action of AMPs

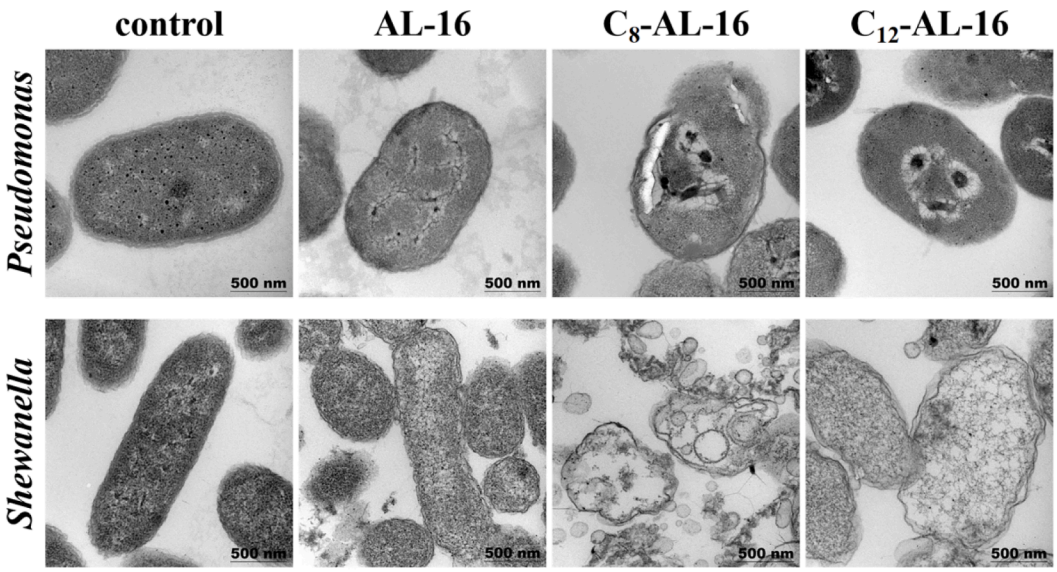

Fig. 5. Morphological changes of bacterial cells following peptide treatment.

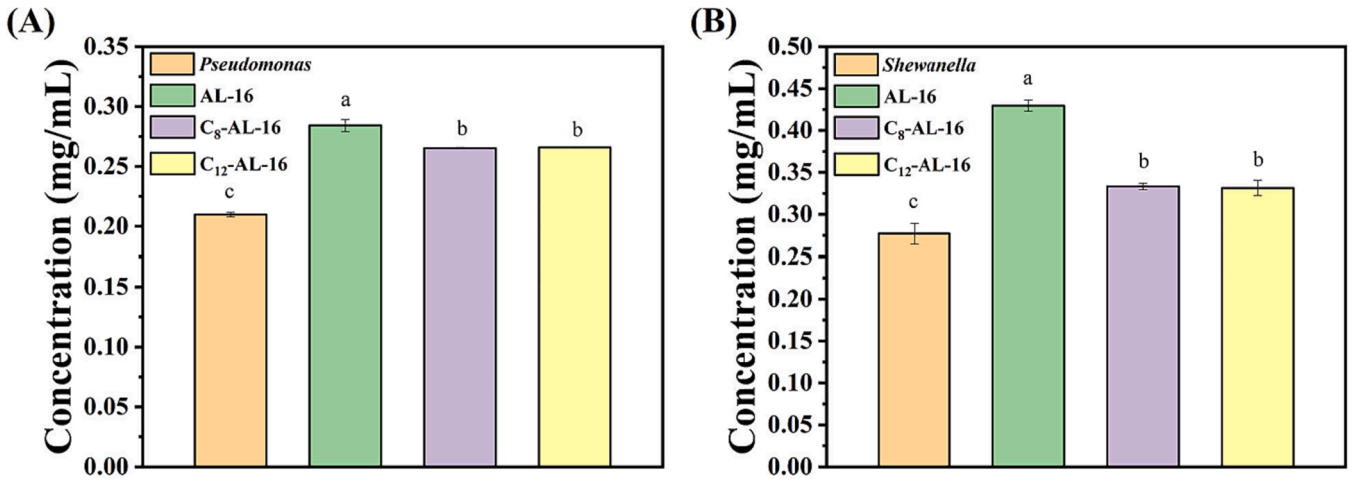

Fig. 6. Protein leakage from the extracellular compartments of *Pseudomonas* (A) and *Shewanella* (B) following treatment with AMPs.

compared to that of the control group, indicating that the cell walls and membranes were damaged, resulting in extracellular leakage of proteins. However, the highest level of extracellular protein leakage was observed in the AL-16-treated group.

The results of the present study indicated that AL-16 induced less damage to bacteria than C_8-AL-16 and C_{12}-AL-16; however, the amount of extracellular protein leakage differed. C_8-AL-16 and C_{12}-AL-16 exhibit potent antibacterial activity, rapidly eliminating bacteria while leading to extracellular protein leakage. However, the antibacterial effect of AL-16 is relatively weak. Bacteria with damaged cell membranes leak extracellular proteins, and some bacteria that were not killed by AL-16 continue to proliferate during the incubation process, resulting in a higher total bacterial count compared to the groups treated with C_8-AL-16 and C_{12}-AL-16. At this stage AL-16 continues to operate, leading to the highest detection of extracellular protein leakage. (Lynes, Zaffuto, Unfricht, Marusov, Samson, & Yin, 2006). Conversely, the hydrophobic nature of the alkyl tail endows the AMP with lytic activity, similar to the surfactant structure of amphiphilic C_8-AL-16 and C_{12}-AL-16 utilizing electrostatic attractions to reach the cell surface in solution. Subsequently, it penetrates the polysaccharide barrier and reaches the outer and inner membranes of gram-negative bacterial cells via an uptake mechanism, reducing the difference between the inner and outer membranes, leading to lysis and cell death (Nasompag, Dechsiri, Hongsing, Phonimdaeng, Daduang, Klaynongsruang, et al., 2015).

3.7. Peptide antimicrobial activity for shrimp bacteriostasis

Litopenaeus vannamei was selected as the experimental material to evaluate the practical applications of AMPs. It is a biologically significant organism with economic and nutritional values. This species is highly susceptible to microbial growth and putrefaction during transportation and storage (Pan, Chen, Hao, & Yang, 2019). Therefore, it is important to suppress the growth of specific organisms that cause spoilage.

Fig. 7 showed the total number of colonies during the fresh-keeping period of *L. vannamei*. The total number of colonies in the sample using AMPs exceeded 6.0 log CFU/g on Day 6, exceeded the microbial limit of food (Herianto, Shih, Lin, Hung, Hsieh, Wu, et al., 2022). The control sample exceeded the safety limit by 4 days. AMPs at the MIC can prolong the shelf life of shrimp by 2 days. On Day 4, the total number of colonies

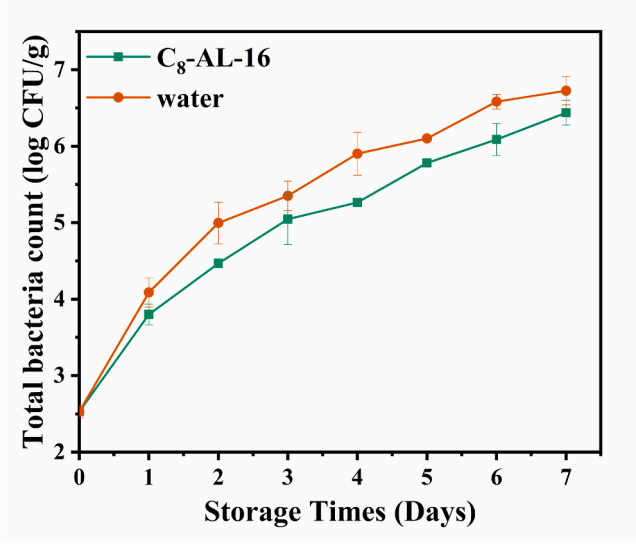

Fig.7. Total bacterial count during the fresh-keeping period of *Litopenaeus vannamei.*

in the control group treated with aseptic water was 0.6 log CFU/g, which was higher than that in the sample treated with AMPs, confirming their antibacterial effect. According to the MIC, the concentration of AMP solution was 7.461 mg/L, and the dosage was very low. Thus, it has application potential owing to its cost-effective and environmental benefits. However, our research is only at the laboratory level and has yet to be tested and verified in large-scale production. The issues related to its effectiveness and dosage still need further exploration.

4. Conclusions

In this study, AP-16 was extracted from sturgeon mucin, and its antimicrobial activity was enhanced through molecular design, resulting in the generation of AL-16, C_8-AL-16, C_{12}-AL-16, and C_{16}-AL-16. Functional activity and safety evaluations resulted in the selection of the antimicrobial peptides AL-16, C_8-AL-16, and C_{12}-AL-16 as the preferred options for storage. Secondary structure analysis revealed that increased length of the alkyl chain promoted the formation of an ordered structure, resulting in reduced MIC and enhanced activity. Changes in the permeability of bacterial cell membranes confirmed the activity of the AMP. TEM results revealed that the AMP caused the lysis and death of *Pseudomonas* and *Shewanella*. Concurrently, we validated AMP activity during shrimp preservation and extended the shelf life of *Litopenaeus vannamei* by 2 days. These results confirmed the inhibitory effect of modified AMPs on the dominant spoilage bacteria of shrimp, supporting their use in antibacterial applications.

CRediT authorship contribution statement

Beining Yang: Writing – original draft, Methodology, Formal analysis, Data curation. **Wei Li:** Validation, Resources, Formal analysis. **Yuxuan Mao:** Visualization, Validation, Investigation, Data curation. **Yuanhui Zhao:** Validation, Formal analysis, Data curation. **Yong Xue:** Resources, Project administration. **Xinxing Xu:** Validation, Supervision. **Yilin Zhao:** Writing – review & editing, Validation, Supervision, Methodology, Formal analysis, Conceptualization. **Kang Liu:** Writing – review & editing, Methodology, Conceptualization.

Declaration of competing interest

The authors declare that they have no known competing financial interests or personal relationships that could have appeared to influence the work reported in this paper.

Data availability

Data will be made available on request.

Acknowledgments

The research was supported by Key R & D Program of Hainan Province (ZDYF2022XDNY191), Science and Technology Support Program of North Jiangsu Province (SZ-LYG202120), Key R & D Program of Shandong Province (2021SFGC0701), Science and Technology Program of Hainan Province (2021CXLH0006) and the opening project of National and Local Joint Engineering Research Center of Deep Processing Technology for Aquatic Products. We would like to thank Editage (www.editage.cn) for English language editing.

Appendix A. Supplementary data

Supplementary data to this article can be found online at https://doi.org/10.1016/j.fochx.2024.101236.

References

Ajish, C., Yang, S., Kumar, S. D., & Shin, S. Y. (2020). Proadrenomedullin N-terminal 20 peptide (PAMP) and its C-terminal 12-residue peptide, PAMP(9–20): Cell selectivity and antimicrobial mechanism. *Biochemical and Biophysical Research Communications, 527*(3), 744–750. https://doi.org/10.1016/j.bbrc.2020.04.063

Al-Sarayreh, S., Al-Shuneigat, J., Al-Saraireh, Y., & Al-Qudah, M. (2021). Effect of Artemisia judaica essential oil on bacterial biofilm and its mode of action. *Journal of Evolution of Medical and Dental Sciences-Jemds, 10*(23), 1777–1783. https://doi.org/10.14260/jemds/2021/367

Ambrosio, R. L., Gogliettino, M., Agrillo, B., Proroga, Y. T. R., Balestrieri, M., Gratino, L., Cristiano, D., Palmieri, G., & Anastasio, A. (2022). An active peptide-based packaging system to improve the freshness and safety of fish products: A case study. *Foods, 11*(3), 338.

Aschi, M., Perini, N., Bouchernal, N., Luzi, C., Savarin, P., Migliore, L., Bozzi, A., & Sette, M. (2020). Structural characterization and biological activity of Crabrolin peptide isoforms with different positive charge. *Biochimica Et Biophysica Acta-Biomembranes, 1862*(2). https://doi.org/10.1016/j.bbamem.2019.183055

Avitabile, C., D'Andrea, L. D., & Romanelli, A. (2014). Circular Dichroism studies on the interactions of antimicrobial peptides with bacterial cells. *Scientific Reports, 4*. https://doi.org/10.1038/srep04293

Bemis, W. E., & Kynard, B. (1997). Sturgeon rivers: An introduction to acipenseriform biogeography and life history. *Environmental Biology of Fishes, 48*(1–4), 167–184. https://doi.org/10.1023/a:1007312524792

Browne, K., Chakraborty, S., Chen, R. X., Willcox, M. D. P., Black, D. S., Walsh, W. R., & Kumar, N. (2020). A New Era of Antibiotics: The Clinical Potential of Antimicrobial Peptides. *International Journal of Molecular Sciences, 21*(19). https://doi.org/10.3390/ijms21197047

Dash, S., Das, S. K., Samal, J., & Thatoi, H. N. (2018). Epidermal mucus, a major determinant in fish health: A review. *Iranian Journal of Veterinary Research, 19*(2), 72–81.

de Almeida, N. R., Han, Y. C., Perez, J., Kirkpatrick, S., Wang, Y. L., & Sheridan, M. C. (2019). Design, Synthesis, and Nanostructure-Dependent Antibacterial Activity of Cationic Peptide Amphiphiles. *Acs Applied Materials & Interfaces, 11*(3), 2790–2801. https://doi.org/10.1021/acsami.8b17808

Garcia, R., Botet, J., Rodriguez-Pena, J. M., Bermejo, C., Ribas, J. C., Revuelta, J. L., Nombela, C., & Arroyo, J. (2015). Genomic profiling of fungal cell wall-interfering compounds: Identification of a common gene signature. *Bmc Genomics, 16*. https://doi.org/10.1186/s12864-015-1879-4

Habtewold, T., Duchateau, L., & Christophides, G. K. (2016). Flow cytometry analysis of the microbiota associated with the midguts of vector mosquitoes. *Parasites & Vectors, 9*. https://doi.org/10.1186/s13071-016-1438-0

Herianto, S., Shih, M. K., Lin, C. M., Hung, Y. C., Hsieh, C. W., Wu, J. S., Chen, M. H., Chen, H. L., & Hou, C. Y. (2022). The effects of glazing with plasma-activated water generated by a piezoelectric direct discharge plasma system on whiteleg shrimp (Litopenaeus vannamei). *Lwt-Food Science and Technology, 154*. https://doi.org/10.1016/j.lwt.2021.112547

Hiraoka, Y., & Kimbara, K. (2002). Rapid assessment of the physiological status of the polychlorinated biphenyl degrader Comamonas testosteroni TK102 by flow cytometry. *Applied and Environmental Microbiology, 68*(4), 2031–2035. https://doi.org/10.1128/aem.68.4.2031-2035.2002

Hussein, W. M., Skwarczynski, M., & Toth, I. (2020). An Isodipeptide Building Block for Microwave-Assisted Solid-Phase Synthesis of Difficult Sequence-Containing Peptides. *Methods in molecular biology (Clifton, N.J.), 2103*, 139–150. https://doi.org/10.1007/978-1-0716-0227-0_9

Kocourkova, L., Novotna, P., St'ovickova-Habartova, L., Cujova, S., Cerovsky, V., Urbanova, M., & Setnicka, V. (2016). Vibrational and electronic circular dichroism

as powerful tools for the conformational analysis of cationic antimicrobial peptides. *Monatshefte Fur Chemie, 147*(8), 1439–1445. https://doi.org/10.1007/s00706-016-1807-6

Kunitake, T. (1992). SYNTHETIC BILAYER-MEMBRANES - MOLECULAR DESIGN, SELF-ORGANIZATION, AND APPLICATION. *Angewandte Chemie-International Edition in English, 31*(6), 709–726. https://doi.org/10.1002/anie.199207091

London, N. J. M., Contractor, H., Lake, S. P., Aucott, G. C., Bell, P. R. F., & James, R. F. L. (1990). A fluorometric viability assay for single human and rat islets. *Hormone and Metabolic Research, 25*, 82–87.

Lynes, M. A., Zaffuto, K., Unfricht, D. W., Marusov, G., Samson, J. S., & Yin, X. Y. (2006). The physiological roles of extracellular metallothionein. *Experimental Biology and Medicine, 231*(9), 1548–1554. https://doi.org/10.1177/153537020623100915

Ma, L., Huang, S. J., Xie, H., Ma, P. P., Jia, B., Yao, Y. F., Gao, Y. X., Li, W. Y., Song, J. J., & Zhang, W. (2022). Influence of chain length on the anticancer activity of the antimicrobial peptide CAMEL with fatty acid modification. *European Journal of Medicinal Chemistry, 239*. https://doi.org/10.1016/j.ejmech.2022.114557

Magana, M., Pushpanathan, M., Santos, A. L., Leanse, L., Fernandez, M., Ioannidis, A., Giulianotti, M. A., Apidianakis, Y., Bradfute, S., Ferguson, A. L., Cherkasov, A., Seleem, M. N., Pinilla, C., de la Fuente-Nunez, C., Lazaridis, T., Dai, T. H., Houghten, R. A., Hancock, R. E. W., & Tegos, G. P. (2020). The value of antimicrobial peptides in the age of resistance. *Lancet Infectious Diseases, 20*(9), E216–E230. https://doi.org/10.1016/s1473-3099(20)30327-3

Nadgir, C. A., & Biswas, D. A. (2023). Antibiotic resistance and its impact on disease management. *Cureus Journal of Medical Science, 15*(4). https://doi.org/10.7759/cureus.38251

Nasompag, S., Dechsiri, P., Hongsing, N., Phonimdaeng, P., Daduang, S., Klaynongsruang, S., Camesano, T. A., & Patramanon, R. (2015). Effect of acyl chain length on therapeutic activity and mode of action of the C-X-KYR-NH2 antimicrobial lipopeptide. *Biochimica Et Biophysica Acta-Biomembranes, 1848*(10), 2351–2364. https://doi.org/10.1016/j.bbamem.2015.07.004

OuYang, Q. L., Duan, X. F., Li, L., & Tao, N. G. (2019). Cinnamaldehyde exerts its antifungal activity by disrupting the cell wall integrity of Geotrichum citri-aurantii. *Frontiers in Microbiology, 10*. https://doi.org/10.3389/fmicb.2019.00055

Pan, C., Chen, S. J., Hao, S. X., & Yang, X. Q. (2019). Effect of low-temperature preservation on quality changes in Pacific white shrimp, Litopenaeus vannamei: A review. *Journal of the Science of Food and Agriculture, 99*(14), 6121–6128. https://doi.org/10.1002/jsfa.9905

Pazderkova, M., Malon, P., Zima, V., Hofbauerova, K., Kopecky, V., Kocisova, E., Pazderka, T., Cerovsky, V., & Bednarova, L. (2019). Interaction of Halictine-Related Antimicrobial Peptides with Membrane Models. *International Journal of Molecular Sciences, 20*(3). https://doi.org/10.3390/ijms20030631

Pulingam, T., Parumasivam, T., Gazzali, A. M., Sulaimana, A. M., Chee, J. Y., Lakshmanan, M., Chin, C. F., & Sudesh, K. (2022). Antimicrobial resistance: Prevalence, economic burden, mechanisms of resistance and strategies to overcome. *European Journal of Pharmaceutical Sciences, 170*. https://doi.org/10.1016/j.ejps.2021.106103

Rawson, K. M., Lacey, M. M., Strong, P. N., & Miller, K. (2022). Improving the therapeutic index of Smp24, a venom-derived antimicrobial peptide: Increased activity against gram-negative bacteria. *International Journal of Molecular Sciences, 23*(14). https://doi.org/10.3390/ijms23147979

Saeed, S. I., Mergani, A., Aklilu, E., & Kamaruzzman, N. F. (2022). Antimicrobial Peptides: Bringing Solution to the Rising Threats of Antimicrobial Resistance in Livestock. *Frontiers in Veterinary Science, 9*. https://doi.org/10.3389/fvets.2022.851052

Sarkar, T., Chetia, M., & Chatterjee, S. (2021). Antimicrobial peptides and proteins: From nature's reservoir to the laboratory and beyond. *Frontiers in Chemistry, 9*. https://doi.org/10.3389/fchem.2021.691532

Song, W., Xin, J. Y., Yu, C., Xia, C. G., & Pan, Y. (2023). Alkyl ferulic acid esters: Evaluating their structure and antibacterial properties. *Frontiers in Microbiology, 14*. https://doi.org/10.3389/fmicb.2023.1135308

Spencer, S. E. F., & Rodger, A. (2021). Bayesian inference assessment of protein secondary structure analysis using circular dichroism data - how much structural information is contained in protein circular dichroism spectra? *Analytical Methods, 13*(3), 359–368. https://doi.org/10.1039/d0ay01645d

Takada, M., Ito, T., Kurashima, M., Matsunaga, N., Demizu, Y., & Misawa, T. (2023). Structure-Activity Relationship Studies of Substitutions of Cationic Amino Acid Residues on Antimicrobial Peptides. *Antibiotics-Basel, 12*(1). https://doi.org/10.3390/antibiotics12010019

Tan, P., Fu, H. Y., & Ma, X. (2021). Design, optimization, and nanotechnology of antimicrobial peptides: From exploration to applications. *Nano Today, 39*. https://doi.org/10.1016/j.nantod.2021.101229

Wang, H. X., Lu, Z. J., Wang, L. J., Guo, T. T., Wu, J. P., Wan, J. Q., Zhou, L. Q., Li, H., Li, Z., Jiang, D. H., Song, P. H., Xie, H. Y., Zhou, L., Xu, X., & Zheng, S. S. (2017). New Generation Nanomedicines Constructed from Self-Assembling Small-Molecule Prodrugs Alleviate Cancer Drug Toxicity. *Cancer Research, 77*(24), 6963–6974. https://doi.org/10.1158/0008-5472.Can-17-0984

Whitmore, L., & Wallace, B. A. (2004). DICHROWEB, an online server for protein secondary structure analyses from circular dichroism spectroscopic data. *Nucleic Acids Research, 32*, W668–W673. https://doi.org/10.1093/nar/gkh371

Winkler, D. F. H. (2020). Automated Solid-Phase Peptide Synthesis. Methods in molecular biology (Clifton. *N.J.), 2103*, 59–94. https://doi.org/10.1007/978-1-0716-0227-0_5

Yamamura, H., Owaki, M., Isshiki, K., Ishihara, Y., Kato, H., Katsu, T., Masuda, K., Osawa, K., & Miyagawa, A. (2023). Anti-bacterial beta-cyclodextrin derivatives inspired by the antimicrobial peptide polymyxin in order to better understand the role of single hydrophobic chain tail in selective anti-bacterial activity. *New Journal of Chemistry, 47*(23), 10921–10929. https://doi.org/10.1039/d3nj01028g

Yan, X. Y., Dong, Y., Dong, T., Song, H. L., Wang, W., & Hu, H. X. (2023). InDel DNA Markers Potentially Unique to Kaluga Sturgeon Huso dauricus Based on Whole-Genome Resequencing Data. *Diversity-Basel, 15*(5). https://doi.org/10.3390/d15050689

Ye, Z., & Aparicio, C. (2019). Modulation of supramolecular self-assembly of an antimicrobial designer peptide by single amino acid substitution: Implications on peptide activity. *Nanoscale Advances, 1*(12), 4679–4682. https://doi.org/10.1039/c9na00498j

Zhao, Y. R., Li, X. F., Zhang, L. M., Wang, D., Wang, W. X., Wang, L., & Chen, C. X. (2020). Tuning the self-assembled nanostructures of ultra-short bola peptides via side chain variations of the hydrophobic amino acids. *Journal of Molecular Liquids, 315*. https://doi.org/10.1016/j.molliq.2020.113765

Zhong, C., Zhang, F. Y., Zhu, N. Y., Zhu, Y. W., Yao, J., Gou, S. H., Xie, J. Q., & Ni, J. M. (2021). Ultra-short lipopeptides against gram-positive bacteria while alleviating antimicrobial resistance. *European Journal of Medicinal Chemistry, 212*. https://doi.org/10.1016/j.ejmech.2020.113138